

ANALYSIS OF THE DYNAMIC LOAD CHARACTERISTICS OF DOUBLE-TOP-BEAM SUPPORTS WITH GAPS

Meng, Z. S.*; Peng, H. X.** & Xie, Y. Y.***,#

* State Key Laboratory of Mining Disaster Prevention and Control Cofounded by Shandong Province and the Ministry of Science and Technology, Shandong University of Science and Technology, 266590 Qingdao, China

** College of Mechanical and Electronic Engineering, Shandong University of Science and Technology, 266590 Qingdao, China

*** College of Civil Engineering and Architecture, Shandong University of Science and Technology, 266590 Qingdao, China

E-Mail: xieyunyue515@sdust.edu.cn (# Corresponding author)

Abstract

Double-top-beam support (DTBS) is an important protective device for backfilling mining. Frequent roof movements cause the DTBS to bear dynamic loads, making it prone to instability and damage. The gaps between the supporting parts exacerbate this condition. To solve this problem, we studied the dynamic characteristics of the DTBS with gaps under various impact loads. Firstly, the numerical model of the support was built. The connecting joints of the DTBS were defined with a gap clearance. Then, the attitude and load characteristics of the DTBS were analysed by applying biased, symmetrical, and torsional load to both top beams. The results indicate that the connecting joints at the top beam are more sensitive to the impact loads. When the impact loads appear at the front part, the load of the connecting bar joints increased. The gap size has a minimal effect on the lateral inclination of the DTBS. The biased loading condition plays a crucial role in the deviation of the top beam supporting attitude. Under the same loading condition, the inclination of the rear top beam is much higher than that of the front top beam, with a degree difference of approximately 130 minutes.

(Received in March 2023, accepted in May 2023. This paper was with the authors 3 weeks for 2 revisions.)

Key Words: Double-Top-Beam Support, Joint Gap Clearance, Attitude Variation, Dynamic Load

1. INTRODUCTION

China has abundant coal resources, and coal is an important chemical energy source that plays a significant supporting role in the country's economic development. The traditional coal mining method is mainly collapse mining. This method is prone to surface subsidence and causes a large amount of coal gangue to accumulate on the surface [1-3]. With the increasing demand for green mining, backfilling mining has become a more widely recommended method. Backfilling mining is the process of refilling the gangue generated during mining into the goaf. To a certain extent, this method has alleviated surface subsidence and reduced the accumulation of surface gangue [4, 5]. Double-top-beam support (DTBS) is mainly used in the backfilling mining process to reduce roof settlement.

During the backfilling process, the impact load received by the DTBS is reduced because of the support effect of backfilling gangue. However, as a result of gaps between the support parts, the DTBS may still bear heavy dynamic loads and exhibit non-ideal bearing attitudes during the loading process [6, 7]. Meanwhile, the presence of gaps caused the impact loads to form exhibit diversity. Therefore, investigating the dynamic performance of the DTBS with gaps under different load forms is necessary, and it contributes to the structural optimization of the DTBS.

2. STATE OF THE ART

In underground mining, complex geological conditions and periodic roof pressure affect the support stability. The frequent cyclic movements of the DTBS cause severe wear at joints. Scholars have conducted extensive research to clarify the factors affecting the performance of the supports. To obtain the static load performance of hydraulic supports, Witek and Prusek [8] used Ansys software to conduct structural statics analysis and dynamics analysis on end hydraulic support, providing a useful way to improve the support static strength. Szurgacz et al. [9] developed a DOH type hydraulic system, and tested the dynamic loads of the support under the external leakage condition during its operation process. Based on the hydraulic support test bench, Stoinski et al. [10] evaluated the dynamic characteristics of the column system. Yang et al. [11] analysed the static load performance of a sliding-type support by establishing the reverse kinematics numerical model; they pointed out that the sliding-type support can achieve strong support for the top plate under low oil pressure. To obtain the dynamic load propagation characteristics of the support, Wang et al. and Xie et al. [12, 13] conducted dynamic simulation and strength analysis, and evaluated the support stability performance.

Guan et al. [14] analysed the influence of column vibration frequency on the support performance of double parallelogram structures; they emphasised that the improved natural frequency has been advanced considerably and the hydraulic support stability has also been significantly improved. By applying different load spectra to the base structure, Xie et al. [15] found that under various impact conditions, the bottom plate specific pressure of hydraulic supports does not exhibit a linear distribution, but rather a V-shaped distribution. Ren et al. [16] proposed an experimental method to examine the dynamic impact of hydraulic supports, designed a 1:2 scaled hydraulic support model, and analysed the load variation under dynamic impact loads; the dynamic response regulation of the support was revealed through experimental data. Zeng et al. [17] used the ZF5600 hydraulic support as an example, established a hydraulic support dynamic model using LS-DYNA, and studied the load variation of hydraulic support under different loading methods. When considering the situation of joint gaps caused by support wear, Zeng et al. [18] analysed the performance of a numerical model of the support with gaps, and then discussed the influence of gap size on the kinematic behaviour of the supports. Wang et al. [19] proposed a virtual simulation concept for hydraulic supports that considers the joint gaps; they analysed the influence of joint gap distribution on the lateral stability of the support and pointed out that the column joint gap has the most significant influence on the support. Bamdad and da Silva et al. [20, 21] studied the effect of joint gaps on machine accuracy by establishing an error model; they concluded that joint gaps have significant influence on the mechanism motion accuracy. Using the dynamic software Adams, Zheng et al. [22] built an impact analysis model for the joint gap of the four-leg support and studied the attitude and dynamic response results of the support. Zhang et al. [23] studied the influence of gap clearance on the dynamic performance of vehicle suspension systems, proposed an optimized control method for gap parameters.

In summary, various factors affect support stability. Compared to the traditional support structure, DTBS has a more complex structure. Therefore, this study takes the DTBS as an example. The dynamic load characteristics of the DTBS were studied by considering factors such as load modes, action positions, and joint clearances.

The rest of this article is arranged as follows. Section 3 analyses equivalent stiffness substitution methods and collision contact modelling methods, as well as loading methods. Section 4 introduces the dynamic variation of the DTBS under various loading methods, and then discusses the attitude variation law. Section 5 provides the conclusion.

3. METHODOLOGY

3.1 Numerical model of the DTBS

In previous research, we established a numerical simulation model for the ideal DTBS model [24]. HyperMesh software was used to build the model and handle the flexible structural parts. The cylinders were defined based on the elastic-spring model. The difference is that in this study, we have arranged connection gaps at each joint. The stiffness definition between the connection gaps can be found in section 3.3. Parts 1–9 indicate the components of DTBS and A–C represent the connecting joints.

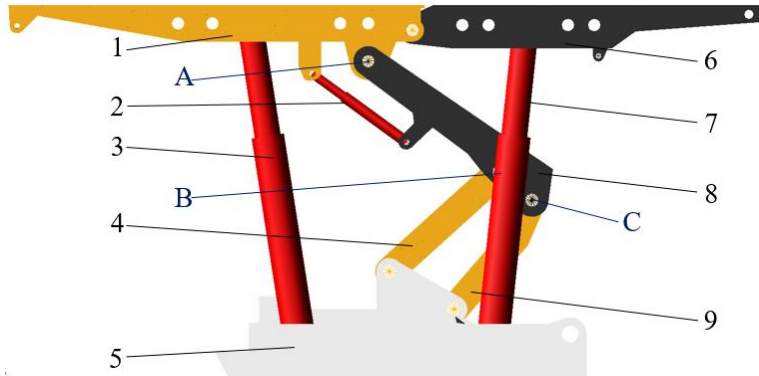


Figure 1: A rigid-flexible coupling analysis model for DTBS.

Fig. 1 shows the model of the target DTBS. The DTBS working height is defined as 3000 mm. The material of the main parts is defined as structural steel. The moving structural components are fully rigid hinged, with the gravity direction set perpendicular to the ground.

3.2 Equivalent replacement for the cylinders

As a support device for underground mining, DTBS requires frequent pushing movements during its operation. The main power source for the support movement process comes from the hydraulic system. In most studies, the hydraulic cylinders of the support are regarded as elastic body with fixed-stiffness or even replaced by a frictional-sliding pair. However, the load act on the support changes dynamically because of periodic roof collapse. The compression amount of the hydraulic cylinder also changes, which means that the stiffness characteristics of the cylinders is continuously changing. To address this issue, we have proposed a variable-stiffness model for hydraulic cylinders. The model is expressed in the following equation [22]:

$$K = \frac{1}{1/K_1 + 1/K_2 + 1/K_3} \quad (1)$$

where K is the calculated stiffness of the target cylinders. Table I lists the calculation parameters of the main DTBS cylinders.

Table I: Calculation parameters of main DTBS cylinders.

Hydraulic cylinder	Diameter of piston cavity (mm)	Diameter of piston rod (mm)	Initial enclosed liquid length (mm)	Piston rod length (mm)
Equilibrium jack	160	105	120	/
Leg	First stage	285	230	970
	Second stage	220	170	990

3.3 Collision model of the DTBS joints

In most studies, researchers regard the support system as a gapless assembly model. However, during the mining process, frequent movement and lifting of the supports inevitably results in joint wear, which leads to the occurrence of connection gaps. However, in most numerical or experimental models, seamless connections are set between the mechanisms, which cannot truly reflect the working state of the supports.

To discuss the impact of joint gaps on the DTBS, this study defines gap collision contacts on each connecting joints. Fig. 2 shows the specific collision model. Adams software is used to calculate the collision contact force expressed as follows.

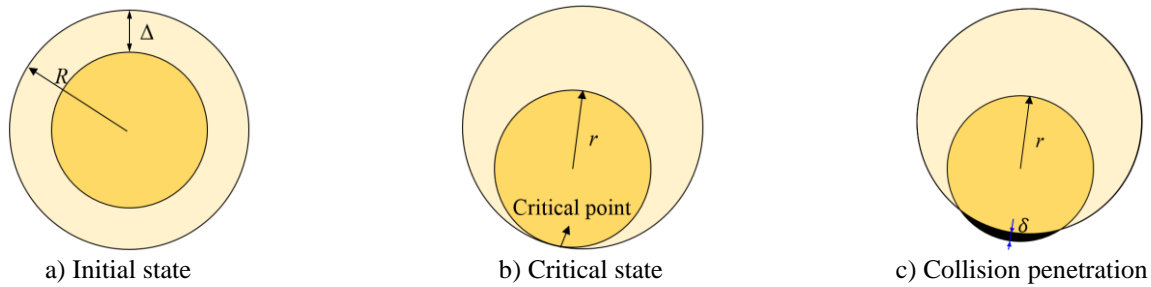


Figure 2: Simplified collision connection model.

$$F_{ni} = K\delta_i^e + CV_i \quad (2)$$

Among them, K , δ , e , C and V represents the calculation stiffness, the penetration depth, the contribution factor, the damping coefficient and the relative velocity, respectively [22].

3.4 Load application method

A static load of 4000 kN is applied to the central place to directly compare the impacts of the dynamic load on the various top beam positions of the DTBS. Three more extreme dynamic loads are set in various positions: loading on both ends, biased loading, and torsional loading. The specific loading form is shown in Fig. 3, where ① the brown loading blocks represent loading at both ends, ② the black loading block is biased loading, and ③ the blue and brown loading blocks represent the torsional loading. The impact load of the black block is 400 kN and that of the other loading blocks is 200 kN. In a single test, the front or rear top beam was loaded separately.

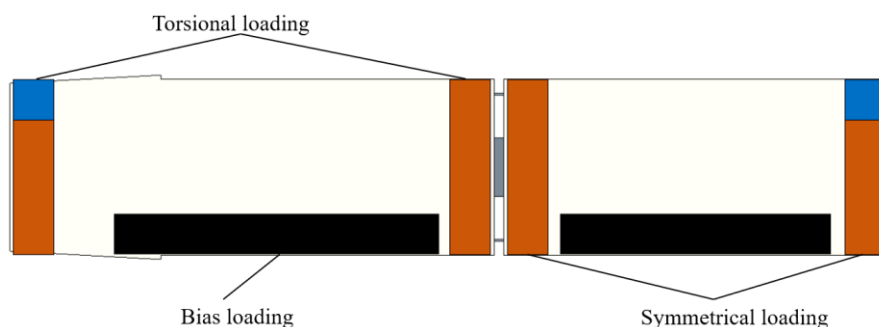


Figure 3: Loading diagram.

4. RESULT ANALYSIS AND DISCUSSION

Compared with ordinary hydraulic supports, the DTBS has a more unique structure. Except for the double-hinged joints between the front top beam (FTB) and rear top beam (RTB), all

other joints are single-hinged connections, which means that a single joint connection may bear excessive load when the impact load occurs. For a more intuitive observation of the results, all load data are presented in the form of histograms. In the graphs, the loading forms are defined as the X axis and the response results are defined as the Y axis. The tangerine, cyan, and violet element represents the dynamic response of the FTB loading condition, RTB loading condition, and various loading conditions, respectively. To facilitate comparison and provide a better description of the results, this section takes the ratio of load difference to load as the load change rate.

4.1 Load variation of the joints between FTB and RTB

The load variation results of the joints between the FTB and RTB are reported in Fig. 4. The figure shows that when the torsional loading is applied, the impact load of the RTB increased the load at the left joint, with a load change rate of 83 %. When the biased loading is applied, the left joint load decreases with a load change rate of 31 %. For the right joint, when the impact load is loaded at both ends, the load on the RTB significantly increases compared to that of the FTB. The load change rate under offset loading reaches approximately 119 %. The effect of the torsional loading method on this point is relatively low, with a change rate of only 3 %. By comparing the load-bearing characteristics, we can find that when the impact load appeared at both ends of the RTB, the joint load increased significantly. Besides, the torsional loading condition of the RTB led to a widening of the load difference between the joints.

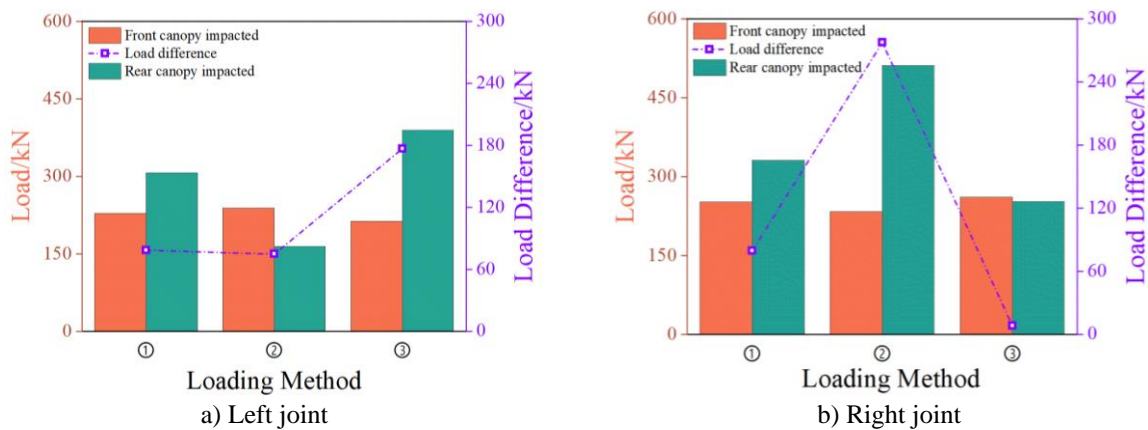


Figure 4: Load variation results of the joints between FTB and RTB.

4.2 Load variation of the joint A

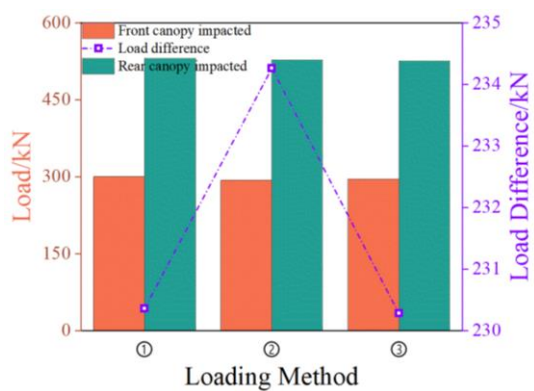


Figure 5: Load variation of the joint A.

Fig. 5 shows the load variation results of joint A. As the figure shows, compared to the ordinary hydraulic supports, the DTBS has a double-top-beam structure that causes the load at joint A to be insensitive when the impact load is applied to the FTB or RTB. When the impact load appears at the RTB, the maximum load change rate reaches 80%. Similarly, the impact loads form variations that have a relatively weak influence on the joint load.

4.3 Load variation of the joint B

Fig. 6 shows the load variation results of joint B. As shown, the loading conditions have less influence on the joint load. Among these loading conditions that appear at the same top beam, the joint load is more sensitive to the biased load. Then, the component loads were compared under the same loading form. The RTB load condition greatly alleviated the joint load, with a maximum load change rate of 89%. This result means that the appearance of this impact load can help reduce the joint load.

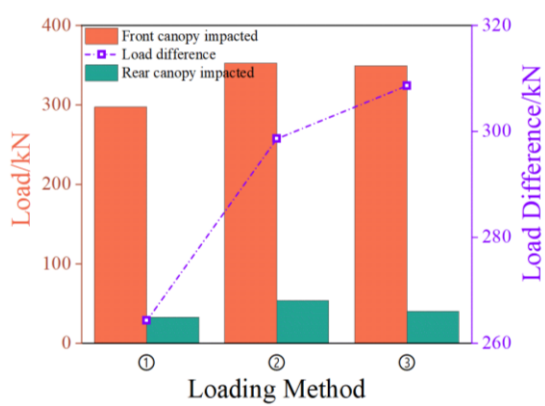


Figure 6: Load variation of the joint B.

4.4 Load variation of the joint C

Fig. 7 shows the load variation results of joint C. For the same component, the influence of loading form changes on the joint load is basically consistent. Among the loading forms, the bias load exhibits a stronger influence, similar to the static analysis of the support. When the impact load appears at the RTB, the joint load is relatively low, with a maximum load change rate of 74%. The change trend of the line chart in the figure indicates that the load change rate is above 70%.

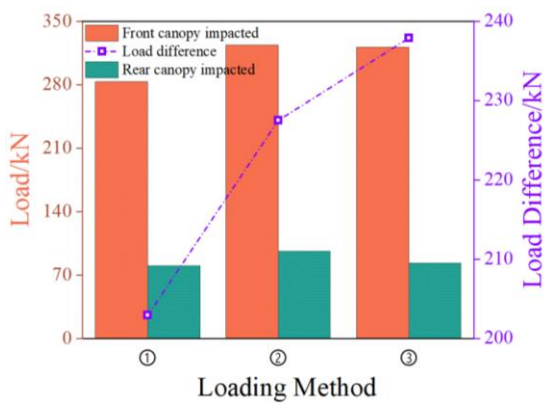


Figure 7: Load variation of the joint C.

A comparison of Figs. 6 and 7 shows that the two hinge joints have a similar sensitivity to various working conditions and loading positions. When the impact load appears at the FTB,

joints B and C share some of the load. When the impact load appears at the RTB, the hinge joints of the FTB side bear a heavier additional load, which means that the RTB does not have a separate equilibrium jack and cannot form an independent bearing structure. Meanwhile, the joint load of the front and rear bars is released to a certain extent. Overall, the joint load are greatly affected by the loading method and the biased load has the greatest influence on the joint load.

4.5 Analysis of FTB and RTB attitudes under two-end loading conditions

As a result of the dynamic working state of underground mining, the joints connecting different components of the support may experience varying degrees of wear. This condition leads to various deformations of the support assembly. Therefore, the DTBS model is established in this part and different gap sizes are defined. The actual assembly state is effectively simulated by replacing the ideal rotating joint with collision contact between the joints. In the following parts, the inclination angles in the four directions of the FTB and RTB are analysed to intuitively express the attitude changes of the FTB and RTB.

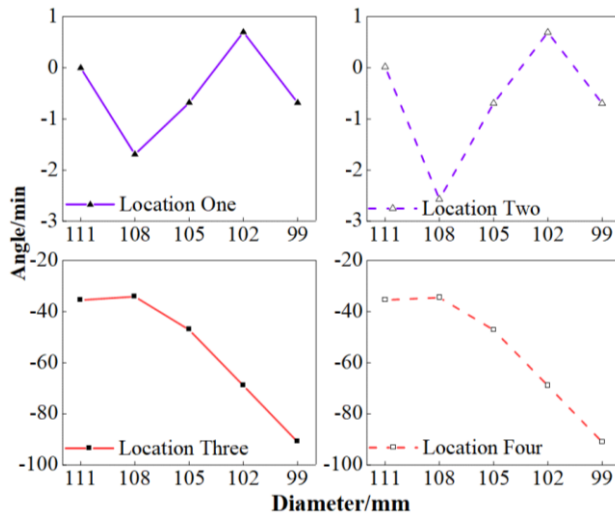


Figure 8: Attitude changes of FTB under loading condition at both ends.

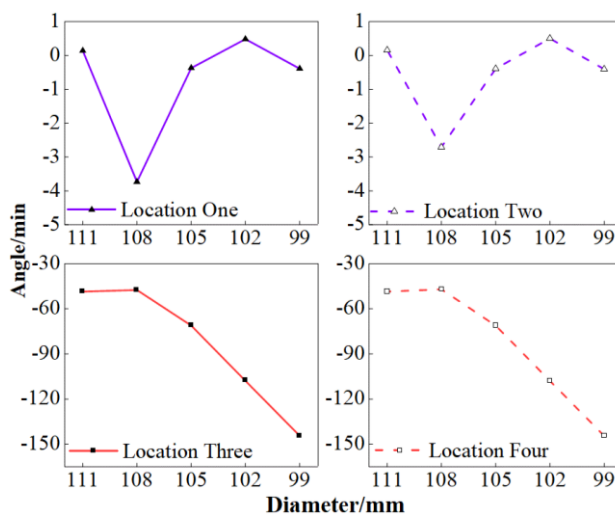


Figure 9: Attitude changes of RTB under the loading condition at both ends.

The attitude changes of the FTB under the loading conditions at both ends is shown in Fig. 8. As the gap size increases, the development trend of the inclination angles of the FTB is

first to decrease, then slightly increases, and then gradually decreases. During this process, the fluctuation amplitude is less than 2.4 minutes. Meanwhile, the development trend of the angles on both sides of the FTB is slightly increase and then gradually decrease, with a fluctuation amplitude of about 57 minutes. It can be noted that the longitudinal attitude of the FTB is greatly affected by the gap size under the loading method at both ends. On the contrary, the lateral attitude fluctuation amplitude of the FTB is small and has lower sensitivity to the gap.

The attitude changes of the RTB under the loading conditions at both ends are shown in Fig. 9. As the gap size increases, the development trend of the inclination angles of the RTB is similar to that of the FTB, which firstly decrease slowly, then increase slightly, and then decrease gradually. However, the fluctuation amplitude is larger than that of the FTB, about 4.2 minutes. The development trend of the longitudinal inclination angle of the RTB is also similar to that of the FTB, with a slight increase and then a gradual decrease, with a fluctuation amplitude of approximately 97 minutes. It can be noted that under the loading method at both ends of the FTB, the influence of the gap sizes on the attitude of the FTB and RTB is similar. The lateral inclination angles of the two top beams exhibit similar fluctuations. As the gap size increases, the longitudinal inclination angles decreases rapidly.

4.6 Analysis of FTB and RTB attitudes under two-end loading conditions

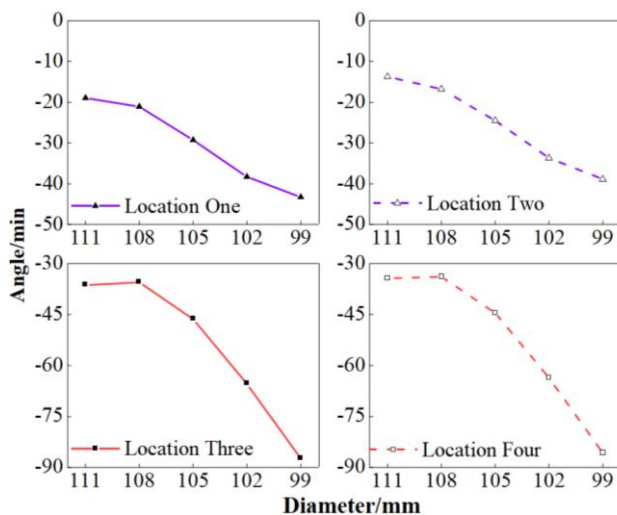


Figure 10: Attitude changes of the FTB under bias loading condition.

Fig. 10 shows the attitude changes of the FTB under the biased loading condition. As the joints gap size increases, the overall development trend of the top beam inclination angles at both ends decreases with a change rate of 25.1 minutes. For the double top beams, the front end leans more sharply than the rear end (show a back tilting attitude). As the joints gap size increases along x-axis, the development trend of FTB longitudinal inclination initially slightly increases, then gradually decreases, with a fluctuation amplitude of approximately 51.9 minutes. From this, it can be seen that under the bias loading method of FTB, compared with the two end loading method, as the hinge gap increases, the lateral tilt posture of FTB becomes more prominent, while the longitudinal tilt degree of FTB decreases.

The attitude changes of the RTB under bias loading conditions are shown in Fig. 11. As the gap size increases, the lateral angle development trend at both ends of the RTB rapidly decreases and then stabilises, with a variation amplitude of approximately 14.4 minutes. The longitudinal inclination angle decreases along the X axis, and the development trend of the FTB inclination angle first slightly increases and then rapidly decreases, with a fluctuation amplitude of approximately 89.2 minutes. These findings show that under the bias loading

method of the FTB, the hinge gap greatly affects the lateral inclination of the RTB. When the pin gap increases to a certain extent, the lateral attitude tends to stabilise, and the longitudinal inclination of the RTB is higher than that of the FTB.

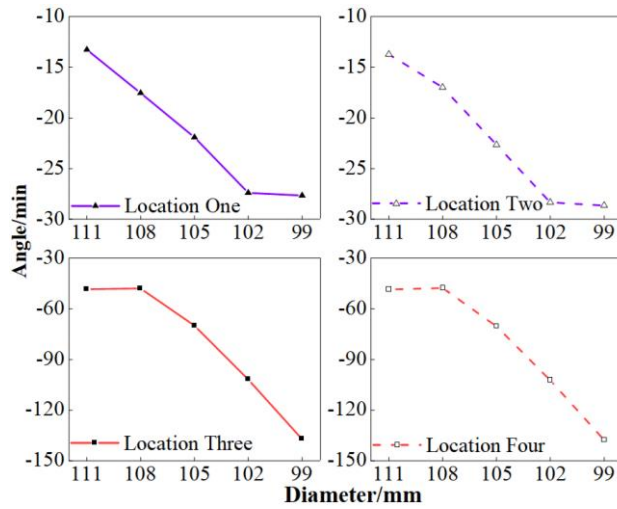


Figure 11: Attitude changes of RTB under bias loading condition.

4.7 Analysis of FTB and RTB attitude under torsional loading condition

Fig. 12 shows the attitude changes of the FTB under torsional loading conditions. The development trend of the lateral angles at both ends of the FTB along the X-axis slowly decreases, then rapidly increases, and then slowly decreases again, with a variation amplitude of approximately 11.3 minutes. Moreover, compared to the front end of the top beam, the rear end part of the support shows a higher inclination degree. In the direction of decreasing the diameter of the pin axis, the development trend of the longitudinal inclination angle of the FTB first increases and then decreases, with a fluctuation amplitude of approximately 56.3 minutes. When the torsional impact load appears at the FTB, the one-side offset load on the front end of the top beam causes the front end to tilt more than the rear end.

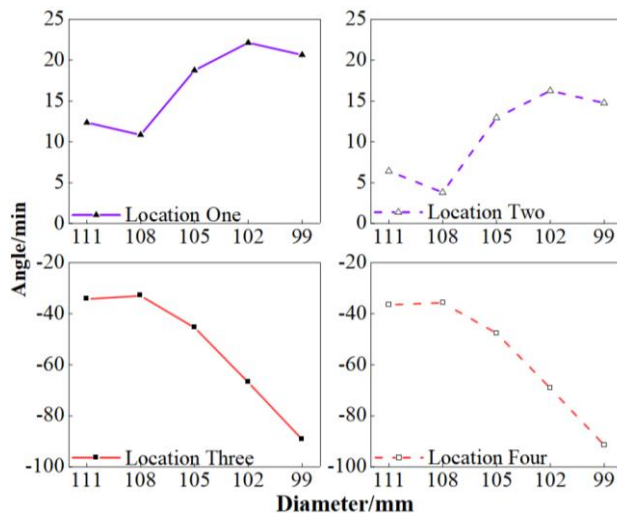


Figure 12: Attitude changes of FTB under torsional loading condition.

The attitude changes of the RTB under torsional loading conditions are shown in Fig. 13. As the joint gap size increases along the X axis, the lateral angle development trend at both ends of the RTB decreases, then increases, and then decreases again, with a variation amplitude of approximately 11.5 minutes. The development trend of the longitudinal

inclination angle of the FTB in the direction of decreasing the diameter of the X axis pin axis shows a smooth transition first, and then a rapid decrease, with a fluctuation amplitude of approximately 96.7 minutes. Overall, the torsional loading method has a weak effect on the attitude symmetry of the RTB. However, the torsional load causes a lateral tilt towards the unloaded side and the longitudinal inclination angle is much higher than that of the FTB.

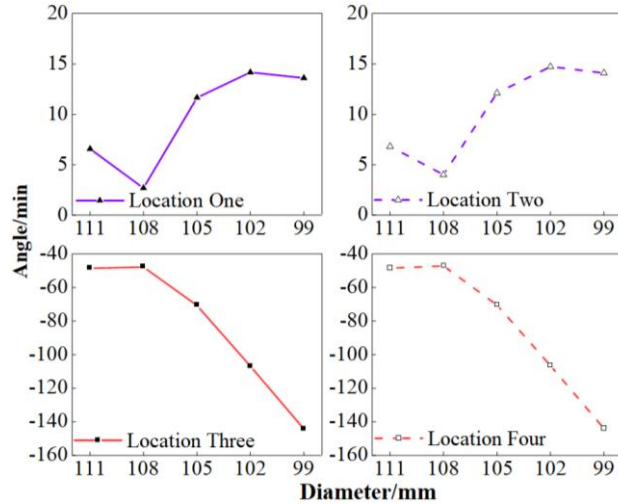


Figure 13: Attitude changes of RTB under torsional loading condition.

In summary, under the loading conditions at both ends of the FTB, the joint gap sizes do not affect the lateral inclination angle of the top beam excessively. The biased loading method causes a certain difference in the lateral inclination angle of the FTB at both ends, and the influence of the joint gap on the lateral inclination angle of the RTB weakens as the gap increases. By comparing the variation patterns of the FTB and RTB under the same loading method, we found that the longitudinal variation trends of the FTB and RTB were similar, but the inclination degree of the RTB was much higher than that of the FTB.

5. CONCLUSION

To analyse the dynamic load characteristics of the DTBS with joint gaps, we built a dynamic numerical model of the DTBS. Then, the impact load in various forms was applied to the DTBS, and the load and attitude changes were obtained. Our findings led to the following conclusions:

(1) When the DTBS was rigidly connected, the hinge joints on both sides of the FTB and RTB had a similar sensitivity to various working conditions and loading positions. When the FTB of the DTBS was subjected to impact loads, joints B and C shared some of the load.

(2) When the DTBS was rigidly connected and the RTB was subjected to impact load, the hinge joint A bore a large amount of additional load, and the load pressure at hinge joints B and C was released to a certain extent. The hinge joints of the FTB and RTB were more sensitive to the impact loads under various loading methods, and their hinge joints on both sides were more greatly affected by offset loads.

(3) Under the loading conditions at both ends of the FTB, the size of the joint gap had a minimal effect on the lateral inclination angle of the top beam. When the impact load was offset loaded, a certain difference was observed in the lateral inclination angle at both ends of the FTB, and the influence of the RTB gap on the lateral inclination angle decreased with the increase of the gap. Moreover, under the same loading method, the longitudinal variation trends of the FTB and RTB were similar, but the inclination degree of the RTB was much higher than that of the FTB.

This study can be a helpful reference for the design and maintenance of DTBS. However, this study only considered the load on a single top beam of the DTBS and only analysed the impact of the gap between two hinge joints on the support. In operating the DTBS, the impact load had a complex and diverse position, and each hinge joint showed varying degrees of wear. The stress response of the DTBS under various hinge-joint gap positions will be analysed in future research.

ACKNOWLEDGEMENT

This work was supported in part by the Natural Science Foundation of China (Grant Nos. 52104164), and the Natural Science Foundation of Shandong Province (Grant Nos. ZR2020QE103).

REFERENCES

- [1] Gong, F. Q.; Zhao, Y. J.; Wang, Y. L.; Peng, K. (2022). Research progress of coal bursting liability indices and coal burst “Human-Coal-Environment” three elements mechanism, *Journal of China Coal Society*, Vol. 47, No. 5, 1974-2010, doi:[10.13225/j.cnki.jccs.2022.0165](https://doi.org/10.13225/j.cnki.jccs.2022.0165)
- [2] Dou, L. M.; Tian, X. Y.; Cao, A. Y.; Gong, S. Y.; He, H.; He, J.; Cai, W.; Li, X. W. (2022). Present situation and problems of coal mine rock burst prevention and control in China, *Journal of China Coal Society*, Vol. 47, No. 1, 152-171, doi:[10.13225/j.cnki.jccs.yg21.1873](https://doi.org/10.13225/j.cnki.jccs.yg21.1873)
- [3] Wang, H. W.; Wang, Q.; Shi, R. M.; Jiang, Y. D.; Tian, Z. (2022). A review on the interaction mechanism between coal bursts and fault structure instability from the perspective of multi-physical field, *Journal of China Coal Society*, Vol. 47, No. 2, 762-790, doi:[10.13225/j.cnki.jccs.XR21.1785](https://doi.org/10.13225/j.cnki.jccs.XR21.1785)
- [4] Pan, Y. S.; Wang, A. W. (2023). Disturbance response instability theory of rock bursts in coal mines and its application, *Geohazard Mechanics*, Vol. 1, No. 1, 1-17, doi:[10.1016/J.GHM.2022.12.002](https://doi.org/10.1016/J.GHM.2022.12.002)
- [5] Waqar, M. F.; Guo, S.; Qi, S. (2023). A comprehensive review of mechanisms, predictive techniques, and control strategies of rockburst, *Applied Sciences*, Vol. 13, No. 6, Paper 3950, 34 pages, doi:[10.3390/app13063950](https://doi.org/10.3390/app13063950)
- [6] Chen, Y.; Zhang, J.; Chen, J.; Deng, X. (2022). Special issue: Rock burst disasters in coal mines, *Energies*, Vol. 15, No. 13, Paper 4846, 6 pages, doi:[10.3390/en15134846](https://doi.org/10.3390/en15134846)
- [7] Yang, Y.; Wei, S.; Li, K. (2021). Inverse analysis of dynamic failure characteristics of roadway surrounding rock under rock burst, *Energy Science & Engineering*, Vol. 9, No. 12, 2298-2310, doi:[10.1002/ese3.977](https://doi.org/10.1002/ese3.977)
- [8] Witek, M.; Prusek, S. (2016). Numerical calculations of shield support stress based on laboratory test results, *Computers and Geotechnics*, Vol. 72, 74-88, doi:[10.1016/j.compgeo.2015.11.007](https://doi.org/10.1016/j.compgeo.2015.11.007)
- [9] Szurgacz, D.; Borska, B.; Zhironkin, S.; Diederichs, R.; Spearing, A. J. S. (2022). Optimization of the load capacity system of powered roof support: a review, *Energies*, Vol. 15, No. 16, Paper 6061, 15 pages, doi:[10.3390/en15166061](https://doi.org/10.3390/en15166061)
- [10] Stoinski, K.; Plonka, M.; Swiatek, J. (2022). Dynamics of large diameter hydraulic legs under applied test methods, *Archives of Mining Sciences*, Vol. 67, No. 2, 259-273, doi:[10.24425/ams.2022.141457](https://doi.org/10.24425/ams.2022.141457)
- [11] Yang, Y.; Zeng, Q.; Zhou, J.; Wan, L.; Gao, K. (2018). The design and analysis of a new slipper-type hydraulic support, *PLoS One*, Vol. 13, No. 8, Paper e0202431, 22 pages, doi:[10.1371/journal.pone.0202431](https://doi.org/10.1371/journal.pone.0202431)
- [12] Wang, D. L.; Zeng, X. T.; Wang, G. F.; Li, R. (2021). Stability of a face guard in a large mining height working face, *International Journal of Simulation Modelling*, Vol. 20, No. 3, 547-558, doi:[10.2507/IJSIMM20-3-572](https://doi.org/10.2507/IJSIMM20-3-572)
- [13] Xie, Y. Y.; Zeng, Q. L.; Jiang, K.; Meng, Z. S.; Li, Q. H.; Zhang, J. M. (2022). Investigation of dynamic behaviour of four-leg hydraulic support under double-impact load, *Strojniski vestnik – Journal of Mechanical Engineering*, Vol. 68, No. 6, 385-394, doi:[10.5545/sv-jme.2022.54](https://doi.org/10.5545/sv-jme.2022.54)
- [14] Guan, E.; Miao, H.; Li, P.; Liu, J.; Zhao, Y. (2019). Dynamic model analysis of hydraulic support, *Advances in Mechanical Engineering*, Vol. 11, No. 1, 8 pages, doi:[10.1177/1687814018820143](https://doi.org/10.1177/1687814018820143)

- [15] Xie, Y. Y.; Meng, Z. S.; Zeng, Q. L.; Yang, C. X.; Gao, K. D. (2020). Analysis of distribution characteristics of study on floor specific pressure of hydraulic support for deep mining based on impact loading, *Journal of China Coal Society*, Vol. 45, No. 3, 982-989, doi:[10.13225/j.cnki.jccs.SJ19.1541](https://doi.org/10.13225/j.cnki.jccs.SJ19.1541)
- [16] Ren, H.; Zhang, D.; Gong, S.; Zhou, K.; Xi, C.; He, M.; Li, T. (2021). Dynamic impact experiment and response characteristics analysis for 1:2 reduced-scale model of hydraulic support, *International Journal of Mining Science and Technology*, Vol. 31, No. 3, 347-356, doi:[10.1016/J.IJMST.2021.03.004](https://doi.org/10.1016/J.IJMST.2021.03.004)
- [17] Zeng, Q.-L.; Li, Z.-J.; Wan, L.-R.; Yang, Y.; Zhu, Y.-P. (2022). Load on bearing and hinge point of hydraulic support under different loading conditions, *Coal Society*, Vol. 54, No. 8, 168-173
- [18] Zeng, Q. L.; Li, Y. Y.; Yang, Y. (2021). Dynamic analysis of hydraulic support with single clearance, *Strojnicki vestnik – Journal of Mechanical Engineering*, Vol. 67, No. 1-2, 53-66, doi:[10.5545/SV-JME.2020.6998](https://doi.org/10.5545/SV-JME.2020.6998)
- [19] Wang, X. W.; Cui, T.; Xie, J. C.; Shen, H. D.; Liu, Y. M.; Wang, B. B. (2022). Virtual simulation method of hydraulic support motion considering pin shaft clearance, *Coal Science and Technology*, Vol. 49, No. 2, 186-193, doi:[10.13199/j.cnki.cst.2021.02.022](https://doi.org/10.13199/j.cnki.cst.2021.02.022)
- [20] Bamdad, M.; Javanfar, A. (2021). Four-bar linkage mechanisms with continuous friction model in joint clearance, *Research Square*, Preprint, 12 pages, doi:[10.21203/rs.3.rs-188389/v1](https://doi.org/10.21203/rs.3.rs-188389/v1)
- [21] Da Silva, M. R.; Marques, F.; da Silva, M. T.; Flores, P. (2022). A comparison of spherical joint models in the dynamic analysis of rigid mechanical systems: ideal, dry, hydrodynamic and bushing approaches, *Multibody System Dynamics*, Vol. 56, No. 3, 221-266, doi:[10.1007/s11044-022-09843-y](https://doi.org/10.1007/s11044-022-09843-y)
- [22] Zeng, Q. L.; Xu, P. H.; Meng, Z. S.; Ma, C.; Lei, X. W. (2023). Posture and dynamics analysis of hydraulic support with joint clearance under impact load, *Machines*, Vol. 11, No. 2, Paper 159, 17 pages, doi:[10.3390/MACHINES11020159](https://doi.org/10.3390/MACHINES11020159)
- [23] Zhang, J.; Chen, Z.; Wang, J.; Hu, Y. (2021). Dynamic characteristics of non-smooth suspension system under fractional-order displacement feedback, *Dyna*, Vol. 96, No. 3, 322-328, doi:[10.6036/10125](https://doi.org/10.6036/10125)
- [24] Meng, Z. S.; Zhang, J. M.; Xie, Y. Y.; Lu, Z. G.; Zeng, Q. L. (2021). Analysis of the force response of a double-canopy hydraulic support under impact loads, *International Journal of Simulation Modelling*, Vol. 20, No. 4, 766-777, doi:[10.2507/IJSIMM20-4-CO18](https://doi.org/10.2507/IJSIMM20-4-CO18)